# Color and Conductivity in $Cu_2O$ and $CuAlO_2$: A Theoretical Analysis of $d^{10}\cdots d^{10}$ Interactions in Solid-State Compounds

Antonio Buljan

*Departamento de Físico-Química, Facultad de Ciencias Químicas, Universidad de Concepción, Casilla 160-C, Concepción, Chile*

Miquel Llunell, Eliseo Ruiz, and Pere Alemany*

*Departament de Química Física, Departament de Química Inorgànica, and Centre de Recerca en Química Teòrica, Universitat de Barcelona, Diagonal 647, 08028 Barcelona, Catalunya, Spain*

*Received August 3, 2000. Revised Manuscript Received October 23, 2000*

The influence of homoatomic $d^{10}\cdots d^{10}$ interactions in the structural and physical properties of some copper-containing oxides has been investigated by using semiempirical band structure calculations of the extended Hückel type. Comparison of the band structures of $CuAlO_2$ and $Cu_2O$, two compounds with Cu(I) ions in practically identical coordination environments, reveals that the spatial arrangement of Cu···Cu contacts is responsible for their markedly different electrical and optical properties. The three-dimensional net of short Cu···Cu distances present in $Cu_2O$ is found to be essential for the appearance of color in this p-type semiconductor. In doped $CuAlO_2$, on the contrary, the 2-D nature of the array of Cu···Cu contacts leads to optical transparency and a lower conductivity if compared to cuprite.

Although optical transparency and electric conductivity seem to be two contradictory physical properties of solids, there are a few known transparent conducting oxides (TCOs) that have been proposed for a large variety of technological applications. TCOs such as doped indium tin oxide (ITO), ZnO, or $SnO_2$ are been used as transparent electrodes in flat panel displays and solar conversion devices.[1,2]The search for new compounds with higher transparency and/or better conductivity than those of the commercially available materials is, however, requested in the development of photoelectronic devices with higher functions. Surprisingly, all studied TCOs are n-type (electron) conductors, while no transparent oxide exhibiting a high p-type (hole) conductivity is known to exist. This new type of material could open the way to some novel applications for TCOs: A combination of the two types of transparent conductors forming a pn junction has been suggested for the construction of functional windows that would transmit visible light while generating electricity in response to absorption of ultraviolet photons, ultraviolet-emitting diodes, or transparent transistors.[3,4]

In a recent paper by Kawazoe et al.,[3] $CuAlO_2$ has been proposed as a starting candidate in the search for new p-type TCOs. The existence of weak homoatomic $d^{10}\cdots d^{10}$ interactions in this compound has been suggested by these researchers as a key factor in determining its optical and electronic properties. To gain a deeper insight into the necessary requirements to obtain better p-type TCOs, we compare here the electronic structures of $CuAlO_2$ and of $Cu_2O$, two $Cu^+$-containing oxides that present weak homoatomic $d^{10}\cdots d^{10}$ interactions. Although both compounds exhibit p-type conduction when properly doped, $CuAlO_2$ is transparent while $Cu_2O$ is strongly colored. The study of the electronic structure of both compounds by the semiempirical extended Hückel method (see the Appendix for more details) reveals the important role of weak $d^{10}\cdots d^{10}$ interactions in the origin of color and conductivity for this family of compounds.

**Structural and Chemical Requirements for Wide-Gap Conductors.** Most oxides of main-group elements such as $SiO_2$ or $Al_2O_3$ are electrical insulators because of their wide band gaps. The considerable ionic character of the cation−oxygen bonding implies deep-lying O(2p) energy levels, which constitute the upper edge of the valence band, and hence wide band gaps for this type of materials. On the other hand, many transition metal oxides behave as semiconductors, although often they are intensely colored because of the existence of intraatomic excitations.

The basic requirements for obtaining good transparent conductors have been recently given by Kawazoe et al.[3,5,6]and will be briefly revised here. Two necessary

(1) Chopra, K. L.; Major, S.; Pandya, D. K. *Thin Solid Films* **1983**, *102*, 1.
(2) Hamberg, I.; Granqvist, C. G. *J. Appl. Phys.* **1986**, *60*, R123.
(3) Kawazoe, H.; Yasukawa, M.; Hyodo, H.; Kurita, M.; Yanagi, H.; Hosono, H. *Nature* **1997**, *389*, 939.
(4) Kudo, A.; Yanagi, H.; Hosono, H.; Kawazoe, H. *Appl. Phys. Lett.* **1998**, *73*, 220.
(5) Kawazoe, H.; Ueda, N.; Un'no, H.; Omata, T.; Hosono, H.; Tanoue, H. *J. Appl. Phys.* **1994**, *76*, 7935.

10.1021/cm001153o CCC: $20.00 © 2001 American Chemical Society
Published on Web 01/12/2001

conditions must be satisfied for obtaining a wide gap conductor. The first one is related to the mobility of carriers. In many electrical insulators the low mobility of carriers, in addition to the large band gap, is the origin of their insulating behavior. For these compounds, conductivity is not expected to be enhanced by doping. The second basic requirement is related to the possibility of carrier generation by properly doping the parent compounds. Since it is difficult to predict from a theoretical point of view how a compound must be doped for efficient generation of charge carriers, we will focus our attention on the first requirement, the high mobility of these carriers, which can be associated with the presence of wide conduction or valence bands for n- and p-type conductors, respectively.

An essential component for an n-type wide-gap conductor is a heavy main-group cation with an $s^0$ electronic configuration. $Zn^{2+}$, $Cd^{2+}$, $Ga^{3+}$, and $In^{3+}$ are, therefore, good candidates for forming oxides in which the bottom edge of the conduction band is composed mainly of s orbitals of the cationic species. Together with this requirement, a wide conduction band, arising from direct overlap between s orbitals on neighboring cations, is necessary to ensure high mobility of conduction electrons. Short M···M distances have been identified as a basic ingredient in the design of n-type TCOs. Structural motifs that accomplish this condition are the linear chains of edge-sharing $MO_6$ octahedra found in the rutile structure of $SnO_2$ or the linear chains of edge-sharing polyhedra present in the case of $In_2O_3$. Vertex-sharing polyhedra with linear M-O-M fragments, on the contrary, give rise to flat bands, inappropriate for high-mobility electron carriers.

The case of p-type TCOs is somewhat different. In these compounds, wide bands at the upper edge of the valence band enhance the mobility of hole carriers. The strong localization of these levels in most of the oxides, where the upper part of the valence band is mainly due to O(2p) levels, may be the reason for the nonexistence of p-type TCOs. The necessary modification of this situation requires the introduction of cations with a closed shell whose energy is comparable to the O(2p) levels. The closed shell is necessary to ensure that no intraatomic excitations will color the crystal. Good candidates for p-type TCOs can be expected for $Cu^+$-, $Ag^+$-, and $Au^+$-containing oxides. Tetrahedral coordination of the oxygen atoms is important to reduce the localized behavior of 2p electrons because there is no nonbonding lone pair left on them.

The crystal structure is also fundamental in the design of a compound with the desired properties. $CuAlO_2$ and $Cu_2O$ contain both $Cu^+$ ions forming linear O-Cu-O fragments and tetrahedrally coordinated O atoms, and when properly doped, both behave as p-type conductors. Their optical properties are, however, totally different: while $CuAlO_2$ is practically transparent with a direct band gap of approximately 3.5 eV[3] (experimental data[7] show, however, that the indirect band gap may be smaller), $Cu_2O$ is strongly colored with a direct band gap of 2.17 eV determined by optical absorption.[8] To understand the origin of the different behavior found for these two compounds, we will start by having a closer look at both crystal structures.

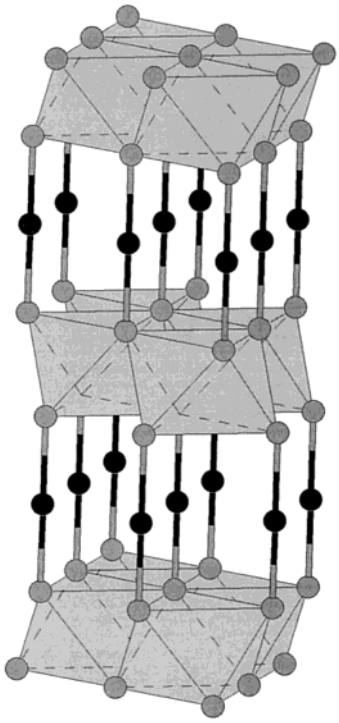

**Figure 1.** Delafossite crystal structure for $CuAlO_2$ (2H polymorph). Cu, black balls; O, gray balls. Al atoms are located in the center of the shaded octahedra.

**Comparison between the Delafossite and the Cuprite Crystal Structures.** Delafossite-type $CuAlO_2$ crystallizes in a simple structure[9] (Figure 1) built of infinite one-octahedron-thick sheets of close-packed $AlO_6$ octahedra. These layers are linked together by the Cu atoms, forming linear O-Cu-O units. Although the stacking of successive layers of $AlO_6$ octahedra can result in different polymorphs, optical and electrical properties,[7,10−12]dominated by the O-Cu-O fragments, are very similar in the two most common polymorphs of $CuAlO_2$, known as 3R[13] and 2H.[14] Oxygen atoms in the delafossite structure have all tetrahedral coordination spheres formed by one copper and three aluminum atoms.

$Cu_2O$ crystallizes in the cuprite structure[9] (Figure 2), formed by a bcc array of oxygen atoms with the copper atoms inserted between two consecutive oxygen layers, in such a way that each oxygen atom is surrounded by a tetrahedron of copper atoms. Each copper atom is two-coordinate, forming linear O-Cu-O units analogous to those found in the delafossite structure. An alternative description of the cuprite structure,[15] which will be used later on, is that it is formed by two interpenetrating frameworks, each one equivalent to the cristobalite

(6) Kawazoe, H.; Ueda, K. *J. Am. Ceram. Soc.* **1999**, *82*, 3330.
(7) Benko, F. A.; Koffyberg, F. P. *J. Phys. Chem. Solids* **1984**, *45*, 57.
(8) Nikitine, S.; Grun, J. B.; Sieskind, M. *J. Phys. Chem. Solids* **1961**, *27*, 931.
(9) Wells, A. F. *Structural Inorganic Chemistry*, 3rd ed.; Clarendon Press: Oxford, U.K., 1984.
(10) Benko, F. A.; Koffyberg, F. P. *Can. J. Phys.* **1985**, *63*, 1386.
(11) Benko, F. A.; Koffyberg, F. P. *Mater. Res. Bull.* **1986**, *21*, 753.
(12) Benko, F. A.; Koffyberg, F. P. *J. Phys. Chem. Solids* **1987**, *48*, 431.
(13) Ishiguro, T.; Kitazawa, A.; Mizutani, N.; Kato, M. *J. Solid State Chem.* **1981**, *40*, 170.
(14) Köhler, B. U.; Jansen, M. *Z. Kristallogr.* **1983**, *165*, 313.
(15) Müller, U. *Inorganic Structural Chemistry*; Wiley: Chichester, U.K., 1993.

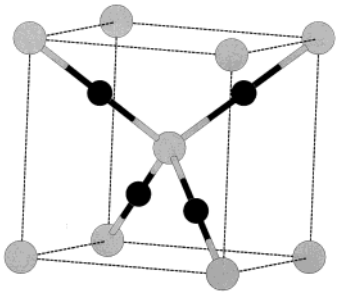

**Figure 2.** Cuprite crystal structure. Cu, black balls; O, gray balls.

structure of $SiO_2$. Figure 3 shows a $2 \times 2 \times 2$ supercell of the cuprite structure in which the two interpenetrating frameworks are represented in different colors.

Since optical and electrical properties of these two compounds are expected to be mainly dominated by the coordination environments of copper atoms, it is important to analyze their geometries carefully. The Cu−O distance in the O-Cu-O fragments is very similar in both compounds: 1.86 Å in $CuAlO_2$ vs 1.85 Å in $Cu_2O$. As far as the second nearest neighbors of copper atoms are concerned, we find interesting differences between them. In the delafossite structure each Cu atom sits in the center of a regular hexagon formed by six copper atoms with a Cu···Cu distance of 2.86 Å. This distance is relatively short when compared with the nearest-neighbor distance found for metallic copper (2.56 Å) and is in the range of intermetallic distances found in copper(I) compounds with weak $d^{10}\cdots d^{10}$ interactions.[16,17] In the cuprite structure each copper atom is surrounded by twelve copper atoms (**1**)

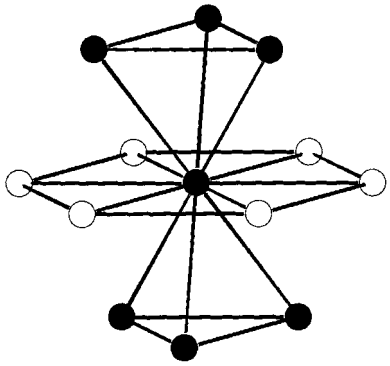

**1**

located at a distance of 3.02 Å. Six of them (black balls in **1**), arranged in a distorted octahedron, belong to the same sublattice as the central copper atom, while the other six (white balls in **1**), which belong to the other sublattice, form a regular hexagon around the central atom. If one compares the two structures, it is evident that while in $CuAlO_2$ copper atoms are arranged in layers, without $d^{10}\cdots d^{10}$ interactions between neighboring layers, in $Cu_2O$, these interactions form a complicated 3-D net of Cu···Cu contacts. As will be seen later, in this compound weak $d^{10}\cdots d^{10}$ interactions are only effective between copper atoms of different sublattices, but even if only these Cu···Cu contacts are considered, the spatial arrangement of Cu···Cu links in the cuprite structure remains still 3-D in nature.

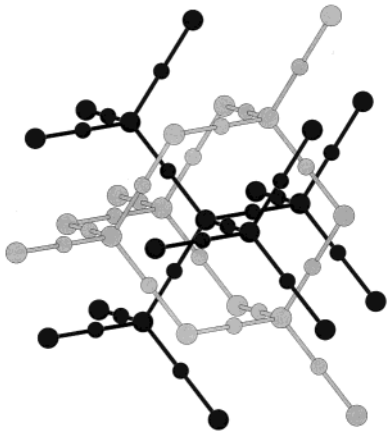

**Figure 3.** Cuprite structure represented as two interpenetrated lattices. Black and gray balls belong to each of the two different sublattices.

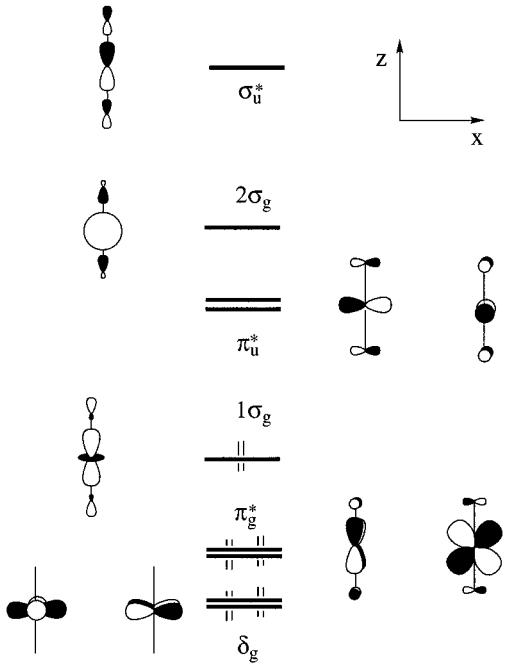


**Figure 4.** Molecular orbitals for a linear $[O\text{-}Cu\text{-}O]^{3-}$ fragment.

**Analysis of the $d^{10}\cdots d^{10}$ Interaction between Linear $[O\text{-}Cu\text{-}O]^{3-}$ Units.** The simplest system that can be used to analyze the $d^{10}\cdots d^{10}$ interactions found in $CuAlO_2$ and in $Cu_2O$ is formed by two linear $[O\text{-}Cu\text{-}O]^{3-}$ units. The relevant MOs for one of these fragments, calculated by the extended Hückel method, are shown in Figure 4. Since interaction between neighboring units is weak, the nature of the valence and conduction bands in both solids will be basically dictated by the orbital ordering shown in the figure. The top of the valence band is thus expected to be formed by the $d_{z^2}$-type orbitals of Cu, which are destabilized by the antibonding interaction with oxygen sp hybrids. The mobility of the carriers that are generated by doping will depend on the dispersion acquired by these orbitals when forming a band through interaction between neighboring copper atoms. Although the relative disposition of neighboring $[O\text{-}Cu\text{-}O]^{3-}$ units is different in both crystals (in $CuAlO_2$ both units are parallel, while in $Cu_2O$ they form a

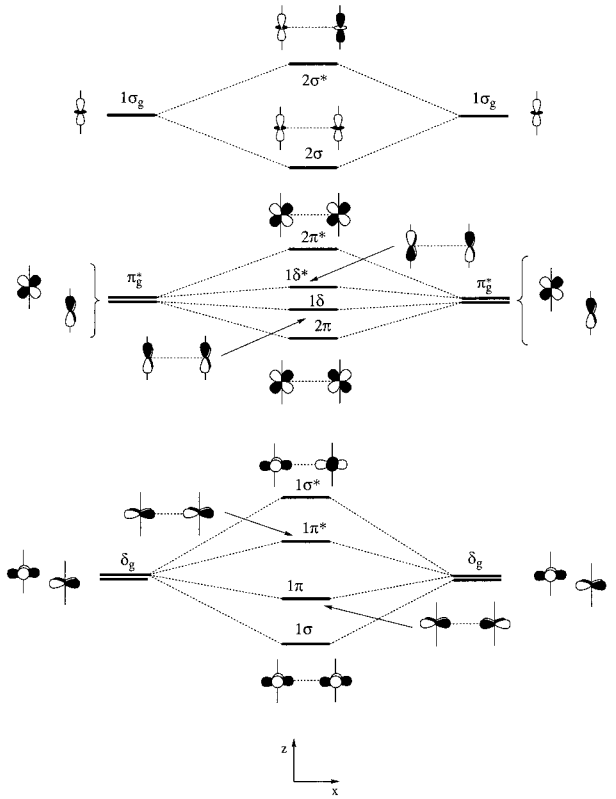


**Figure 5.** Orbital interaction diagram for two parallel $[O\text{-}Cu\text{-}O]^{3-}$ fragments.

dihedral angle of 70.5°), this difference does not affect the dispersion of the band originated from the $d_{z^2}$-type orbitals since their interaction is insensitive to rotations around the Cu···Cu axis. In the following we will discuss only the case of two parallel $[O\text{-}Cu\text{-}O]^{3-}$ fragments as found in $CuAlO_2$.

The interaction diagram for two parallel $[O\text{-}Cu\text{-}O]^{3-}$ fragments is presented in Figure 5. The calculated Cu···Cu overlap population for a Cu···Cu distance of 3.02 Å is 0.0058, indicating a weak bonding interaction between both closed shells. The positive overlap population has been explained by mixing of empty s and p orbitals with the filled d ones.[18,19]In this case, the interaction responsible for the weak bond can be attributed to the 1$\sigma$-1$\sigma$* pair (**2**).

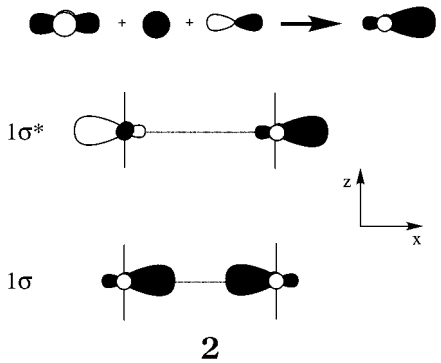


**2**

Mixing of s and p orbitals into the symmetric (1$\sigma$) and antisymmetric (1$\sigma$*) combinations of the $x^2 - y^2$ orbitals leads to an enhanced bonding interaction for 1$\sigma$ and a less antibonding interaction for 1$\sigma$*. To check the role of empty s and p orbitals in the weak $d^{10}\cdots d^{10}$ interaction, one can remove the s and p orbitals from the basis set and recalculate the Cu···Cu overlap population. The result of this numerical experiment gives an overlap population of −0.0004, indicating a net repulsion between both atoms. A detailed analysis of the contribution of each orbital to the overall Cu···Cu overlap population shows that the 1$\sigma$ orbital contributes 0.0184, a value that is not completely canceled by the contribution of the 1$\sigma$* orbital, which is only −0.0094. For the rest of orbitals, the contribution of the bonding and antibonding combinations practically cancel each other, except for the $d_{z^2}$ pair, 2$\sigma$ and 2$\sigma$*, for which hybridization with the empty s and p orbitals results in a slight enhancement of the antibonding interaction with respect to the bonding one. The mobility of the carriers, which will be created in the band originated from the 2$\sigma$* orbitals, will be enhanced by the hybridization that results in an elongation of the "doughnut" of the $d_{z^2}$ orbital in the Cu···Cu direction (**3**), which will result in a reinforcement of the overlap between neighboring units, and therefore in a wider band in the solid.

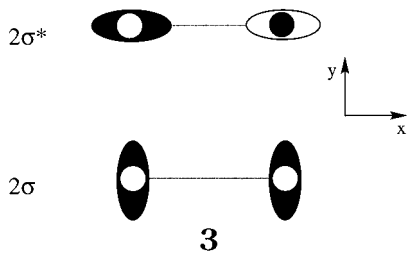


**3**

As already mentioned, the most important features of the $d^{10}\cdots d^{10}$ interaction described above arise from $\sigma$-type orbitals and are insensitive to rotation of the $[O\text{-}Cu\text{-}O]^{3-}$ units around the Cu···Cu axis, making the different relative orientations of the O-Cu-O fragments in $CuAlO_2$ and $Cu_2O$ irrelevant in the following discussion. For constant Cu−O bond distances, the Cu···Cu distance is the only geometrical parameter that plays a key role in determining the strength of the $d^{10}\cdots d^{10}$ interaction. A decrease of this distance from 3.02 to 2.86 Å (the values found in $Cu_2O$ and $CuAlO_2$, respectively) increases the Cu···Cu overlap population from 0.0058 to 0.0128. The bonding and antibonding nature of the 2$\sigma$ and 2$\sigma$* orbitals is also enhanced. A measure of the dispersion of the band that will arise from the $d_{z^2}$ orbitals of copper is given by the energy splitting between the 2$\sigma$ and 2$\sigma$* orbitals, and it increases from 0.18 to 0.25 eV when the Cu···Cu distance is reduced from 3.02 to 2.86 Å.

In $Cu_2O$ 12 copper atoms surround each copper at 3.02 Å, six of them belonging to the same sublattice as the central atom. While the model formed by two $[O\text{-}Cu\text{-}O]^{3-}$ units described above is able to reproduce the essential features of the $d^{10}\cdots d^{10}$ interaction between atoms of different sublattices, the smallest unit required to study the $d^{10}\cdots d^{10}$ interaction between two copper atoms belonging to the same sublattice is given by the angular $[Cu_2O_3]^{4-}$ fragment shown in **4**.

(16) Jansen, M. *Angew. Chem., Int. Ed. Engl.* **1987**, *26*, 1098.
(17) Pyykkö, P. *Chem. Rev.* **1997**, *97*, 597.
(18) Mehrotra, P. K.; Hoffmann, R. *Inorg. Chem.* **1978**, *17*, 2187.
(19) Alemany, P.; Alvarez, S. *Inorg. Chem.* **1992**, *31*, 4266.

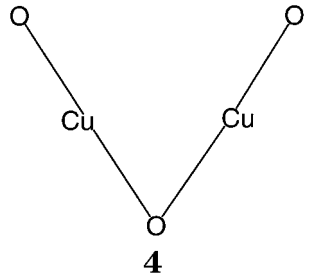


**4**

The calculated Cu···Cu overlap population for this fragment is −0.0036, indicating a net repulsion between both metal atoms. An analysis of the molecular orbitals shows that the reason for this different behavior can be found in the poor overlap between the orbitals of each O-Cu-O fragment, which do not directly point toward each other in the $[Cu_2O_3]^{4-}$ unit, together with an unfavorable hybridization pattern with s and p orbitals. It is important to note that although the Cu···Cu distance is the same in both cases, the weak $d^{10}\cdots d^{10}$ interaction between the two copper atoms has a different sign, depending on the particular geometry of each fragment. This example shows that, in general, a relatively short distance between two atoms is not indicative of the existence of these $d^{10}\cdots d^{10}$ interactions.

**$d^{10}\cdots d^{10}$ Interactions in $CuAlO_2$ and $Cu_2O$.** Figure 6 shows the density of states (DOS) and the Cu···Cu crystal orbital overlap population (COOP) curves in the region of the valence band close to the Fermi level for $CuAlO_2$ (left-hand panel) and $Cu_2O$ (right-hand panel). As expected from our previous discussion, the top of the valence band is mainly associated with bands arising from the $d_{z^2}$-type orbitals of copper (hatched in the figure). The integrated COOP curves indicate a net positive overlap population at the Fermi level for $CuAlO_2$ and for the copper pairs belonging to different sublattices in $Cu_2O$. The actual values for the overlap population, summarized in Table 1, are very similar to those obtained for the discrete fragments studied in the preceding section. A calculation for a modified structure of $CuAlO_2$ in which the Cu···Cu distances are expanded to 3.02 Å gives a reduction in the overlap population similar to that found for two $[O\text{-}Cu\text{-}O]^{3-}$ units. In the solid-state structure, the overlap population between two neighboring Cu atoms on the same sublattice is also found to be negative.

To check the influence of s, p hybridization with the d orbitals in the solid-state structures, the calculations have been repeated with the s and p orbitals of copper omitted from the basis set. The values of the Cu···Cu overlap population (Table 1) show the same trends found for the discrete fragments, indicating that the mechanism already discussed for molecular compounds is also at the origin of $d^{10}\cdots d^{10}$ interactions in extended solid-state structures.

Hybridization of Cu d orbitals with higher energy unoccupied s and p states, as suggested by our calculations, has been recently observed in an experimental study[20] on $Cu_2O$. The analysis of experimental data indicates that about 0.22 electron per atom is removed from copper $d_{z^2}$ states. This finding is in excellent qualitative agreement with the mechanism for $d^{10}\cdots d^{10}$ interactions proposed from our analysis, although the actual figure found from experimental data almost

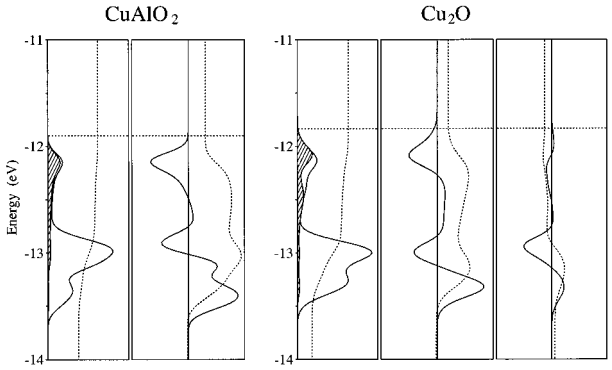


**Figure 6.** Density of states (DOS) and Cu···Cu crystal orbital overlap population (COOP) curves for $CuAlO_2$ and $Cu_2O$. The hatched areas in the DOS plots indicate states arising from $d_{z^2}$-type orbitals of copper. The two COOP curves for $Cu_2O$ correspond to Cu···Cu interactions between different sublattices (left) and to Cu···Cu interactions within the same sublattice (right). Positive values of the COOP curve indicate bonding states; negative ones indicate antibonding states. The dashed curve in the COOP plots corresponds to the integrated COOP curve, and its value at the Fermi level (dashed horizontal line) gives the net overlap population between the pair of atoms considered in each case.

**Table 1. Cu···Cu Overlap Populations in $CuAlO_2$ and $Cu_2O$, Calculated Using All Valence Orbitals on the Copper Atoms (s,p,d) and Only the d-orbital Set (only d).**

| | $d_{Cu-Cu}$ (Å) | ov pop. (s, p, d) | ov pop. (only d) |
|---|---|---|---|
| $CuAlO_2$ | 2.86 | +0.0075 | 0.0009 |
| $Cu_2O$ (same sublattice) | 3.02 | 0.0032 | 0.0003 |
| $Cu_2O$ (between sublattices) | 3.02 | +0.0049 | 0.0004 |

doubles the one obtained in our calculations. The interpretation of the experimental data given by Zuo et al.[20] in their work has, however, been recently questioned by Wang and Schwarz.[21] Acoording to these authors, there seems as yet to exist no proof of significant Cu−Cu closed-shell bonding at such large distances as those found in cuprite. As we will discuss in the next section, the appearance of color in $Cu_2O$ may be seen, in our opinion, as important evidence for the presence of these interactions in this compound.

**Influence of $d^{10}\cdots d^{10}$ Interactions on the Conductivity and Color of $CuAlO_2$ and $Cu_2O$.** The main goal of this work is to analyze the role that the extended net of $d^{10}\cdots d^{10}$ contacts found in delafossite and in cuprite may have in their electrooptical properties. The two main features of the band structure that we will look at are (a) the band gap and (b) the width of the $d_{z^2}$-type bands close to the Fermi level. To allow a direct comparison of our semiempirical calculations for both solids, the band structure of $CuAlO_2$ has been replaced by that of an infinite layer of composition $[CuO_2]^{3-}$. A detailed comparison of the band structure for the complete crystal and that calculated for this slab shows that both are qualitatively equivalent in the region around the Fermi level. Aluminum orbitals have a negligible participation in the valence band of $CuAlO_2$ and therefore do not affect the width of the bands close

(20) Zuo, J. M.; Kim, M.; O'Keeffe, M.; Spence, J. C. H. *Nature* **1999**, *401*, 49−52.
(21) Wang, S.-G.; Schwarz, W. H. E. *Angew. Chem., Int. Ed. Engl.* **2000**, *39*, 1757−1762.

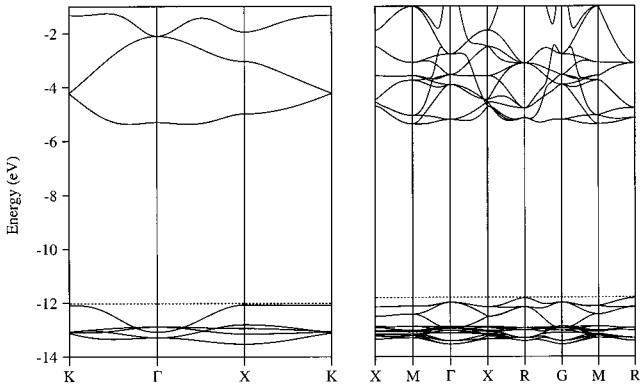


**Figure 7.** Band structures for $[CuO_2]^{3-}$ (left) and $Cu_2O$ (right). The dashed horizontal line indicates the position of the Fermi level. In both compounds, the valence band (centered around −13 eV) is clearly separated from the conduction band (levels above −6 eV) by a band gap.

to the top of the valence band. As far as the gap is concerned, participation of aluminum states at the bottom of the conduction band, even if small, could introduce some differences when compared to $Cu_2O$ that are difficult to evaluate by a semiempirical approach like ours. Since we are interested only in the qualitative variations experienced by the band gap when the strength of Cu···Cu interactions is modified, and not in its accurate value, which the extended Hückel method is not expected to reproduce properly, we think that the model structure adopted for $CuAlO_2$ is sufficient to reproduce all the features of the band structure needed in our discussion. In this way we deal with two systems having the same computational parameters, avoiding the problem of calibrating the effect of the parameters of aluminum in the calculations.

Figure 7 shows the band structure for the $[CuO_2]^{3-}$ slab and for $Cu_2O$. In both cases our calculations predict an indirect gap of approximately 6−7 eV. These values are overestimated with respect to the experimental measurements of this magnitude, although, as said before, we will not be concerned here with the actual values of the band gap, which depend strongly on the atomic parameters adopted in the calculations. What we want to study is the influence of Cu···Cu interactions on the band gap and on the width of the valence band. For a detailed study of the electronic structure of $CuAlO_2$ and $Cu_2O$, the reader is referred to earlier work[22,23]and references therein.

It is very easy to study the influence of the Cu···Cu distance on these magnitudes with the $[CuO_2]^{3-}$ slab. The variation of the band gap with this geometrical parameter is shown in Figure 8. As expected from the decrease of overlap between neighboring copper orbitals, the valence band becomes narrower for separation of the copper atoms. Since the conduction band, mainly formed from copper s and p orbitals, also becomes narrower, the band gap is widened upon increasing the Cu···Cu distance. This finding is in good agreement with the trend found by Jansen[16] for the activation energies in a series of delafossites with varying Cu···Cu distances.

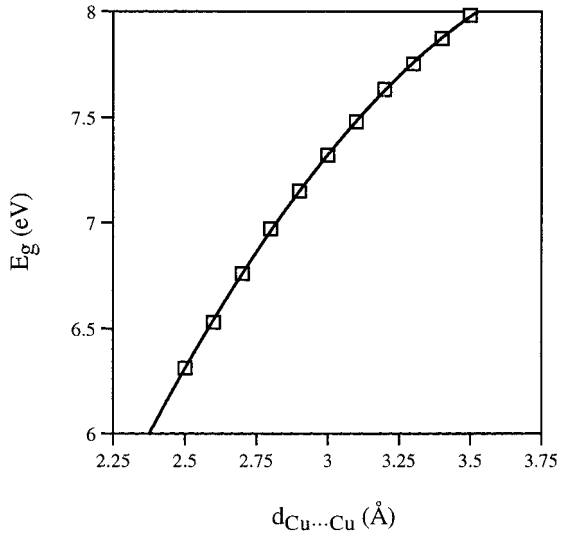


**Figure 8.** Variation of the band gap and the width of the valence band with the Cu···Cu distance in the $[CuO_2]^{3-}$ layer.

**Table 2. Band Gap ($E_g$) and Valence-Band Width ($W$) for $[CuO_2]^{3-}$ and $Cu_2O$**

| | $d_{Cu-Cu}$ (Å) | $E_g$ (eV) | $W$ (eV) | deleted Cu···Cu interactions | $E_g$ (eV) | $W$ (eV) |
|---|---|---|---|---|---|---|
| $[CuO_2]^{3-}$ | 2.86 | 6.70 | 1.45 | all | 8.05 | 0.79 |
| | 3.02 | 7.05 | 1.22 | all | 8.20 | 0.77 |
| $Cu_2O$ | 3.02 | 6.46 | 1.71 | same sublattice | 5.17 | 1.69 |
| | 3.02 | | | between sublattices | 7.17 | 1.24 |

[a] Values in the last two columns correspond to calculations in which neighboring Cu···Cu interactions have been selectively deleted in the Hamiltonian matrix.

If the expected variation of the band gap and the width of the valence band with the Cu···Cu distance is used to compare these properties of $CuAlO_2$ and $Cu_2O$, one would arrive at the wrong conclusion that the gap should be wider in cuprite. In view of this apparent contradiction with experimental observations, a more elaborate explanation must be found for the origin of color in $Cu_2O$. To analyze the effect of $d^{10}\cdots d^{10}$ interactions on the band gap and the width of the valence band we have performed the following numerical experiment: repeat all calculations, deleting the terms in the Hamiltonian matrix that represent interactions between orbitals of two neighboring copper atoms. This procedure works well for weak interactions such as the $d^{10}\cdots d^{10}$ case studied here but must be carefully performed if one wants to study the effect of stronger interactions, since deleting large elements of the Hamiltonian matrix often leads to senseless results. The values for the band gap and the width of the valence band for systems in which $d^{10}\cdots d^{10}$ interactions have been selectively annihilated are reported in Table 2. These data indicate clearly that $d^{10}\cdots d^{10}$ interactions between copper atoms are essential in determining both the band gap and the width of the valence band. When the $d^{10}\cdots d^{10}$ interactions are suppressed, both compounds show similar band gaps. Since the larger Cu···Cu distance in $Cu_2O$ should lead to a narrower band, we must conclude that the key factor in the relatively small band gap (wide valence band) found in cuprite is, as anticipated by Kawazoe et al.,[3] the topology of the 3D arrangement of Cu···Cu contacts that allows much more effective $d^{10}\cdots d^{10}$ interactions than the 2D arrangement

(22) Buljan, A.; Alemany, P.; Ruiz, E. *J. Phys. Chem. B* **1999**, *103*, 8060.
(23) Ruiz, E.; Alvarez, S.; Alemany, P.; Evarestov, R. A. *Phys. Rev. B* **1997**, *56*, 7189.

**Table 3. Atomic Parameters for Extended Hückel Calculations[a]**

| atom | orbital | $H_{ii}$ (eV) | $\zeta_{i1}$ | $c_1$ | $\zeta_{i2}$ | $c_2$ |
|---|---|---|---|---|---|---|
| Cu | 4s | 8.345 | 2.200 | | | |
| | 4p | 4.216 | 2.200 | | | |
| | 3d | 13.162 | 5.950 | 0.5933 | 2.300 | 0.5744 |
| O | 2s | 31.600 | 2.275 | | | |
| | 2p | 16.776 | 2.275 | | | |
| Al | 3s | 11.794 | 1.167 | | | |
| | 3p | 5.976 | 1.167 | | | |

[a] $H_{ii}$ are the valence shell ionization potentials,[28] $\zeta_{ij}$ are the Slater exponents, and $c_j$ are the coefficients in the double-$\zeta$ expansion of the d orbitals.

found in $CuAlO_2$. This finding shows that in this case the physical properties depend not only on local features of the crystal structure but also on its global spatial arrangement.

## Conclusions

Weak $d^{10}\cdots d^{10}$ interactions, which have been previously described for discrete organometallic compounds, are also present in a great number of extended solid-state phases. Together with the important structural implications of these interactions, a detailed analysis of the band structure reveals that they also play a key role in the appearance of color and conductivity in $CuAlO_2$ and $Cu_2O$. It is remarkable, however, that these two properties not only are dependent on local features of $d^{10}\cdots d^{10}$ contacts but also are intimately related to the topology of the network of $d^{10}\cdots d^{10}$ interactions that extend through the whole crystal structure. As a conclusion, 3D arrangements of Cu···Cu contacts should be avoided if one wants to obtain a good p-type transparent conductor based on Cu(I)−O compounds.

**Acknowledgment.** We are grateful to S. Alvarez and E. Canadell for helpful comments on this work. A.B. thanks the *Agencia Española de Cooperación Internacional* for a MUTIS fellowship. Financial support to this work was provided by FONDECYT (Chile) through Grant 3980044, DGES (Spain) through Project PB98-1166-CO2-01, and CIRIT (Generalitat de Catalunya) through Grant SGR99-0046.

## Appendix

All qualitative theoretical discussions presented in this paper are based on molecular orbital[24] and tight-binding band calculations[25,26]of the extended Hückel type as implemented in the CASSANDRA[27] suite of programs. Atomic parameters used in the calculations are those shown in Table 3

CM001153O

(24) Hoffmann, R. *J. Chem. Phys.* **1963**, *39*, 1397.
(25) Whangbo, M.-H.; Hoffmann, R. *J. Am. Chem. Soc.* **1978**, *100*, 6093.
(26) Whangbo, M.-H.; Hoffmann, R.; Woodward, R. B. *Proc. R. Soc. London A* **1979**, *366*, 23.
(27) Llunell, M.; Alemany, P.; Ruiz, E. *CASSANDRA*, v. 0.3; Universitat de Barcelona: Barcelona, Catalunya, Spain, 1999.
(28) Vela, A.; Gázquez, J. L. *J. Phys. Chem.* **1988**, *92*, 5688.